ELSEVIER

Journal of Contaminant Hydrology 23 (1996) 185–211

JOURNAL OF
Contaminant
Hydrology

Contaminant migration in the unsaturated soil zone: the effect of rainfall and evapotranspiration

Jordi Grifoll [a,*], Yoram Cohen [b]

[a] *Departament d'Enginyeria Química, Escola Tècnica Superior d'Enginyeria, Universitat Rovira i Virgili, Tarragona, Spain*

[b] *Department of Chemical Engineering and National Center for Intermedia Transport Research, University of California, Los Angeles, CA 90024, USA*

Received 14 February 1995; accepted 23 August 1995

Abstract

The potential effect of rainfall and evapotranspiration on contaminant migration in the unsaturated soil zone was studied using a deterministic dynamic modeling approach. The contaminant mass transfer equation was solved along with Richards' equation for water transport subject to dynamic surface boundary conditions that consider rainfall and evapotranspiration. As an illustration of the effect of rainfall and evapotranspiration on various transport mechanisms, test cases are presented for the transport and volatilization of benzene, *1,1,2,2*-tetrachloroethane and methanol for a loam-type soil using self-consistent dynamic rainfall and evapotranspiration weather sequences. The present study suggests that transport mechanisms such as diffusion, dispersion and convection can all be significant, to varying degrees, during various parts of the year. The temporal variability of both the volatilization flux and the amount of chemical remaining in the unsaturated soil zone are significantly impacted by the dynamics of rainfall and the period of initial contamination.

1. Introduction

Direct exposure of human and ecological receptors to contaminants present in the soil environment may occur via the inhalation of toxic solutes as they volatilize from the soil, dermal absorption due to contact with the soil, ingestion of soil particles, or from drinking contaminated groundwater. Given the growing concern with the environmental impact of contaminants in the soil environment, a number of different deterministic

* Corresponding author.

SSDI 0169-7722(95)00086-0

transport models have been proposed over the last several decades to describe the movement of chemical contaminants in the vadose soil zone. The simplest models account only for diffusion in a single soil phase (e.g., soil-air, soil-water) and adsorption by the soil-solids, whereas more elaborate models consider the soil matrix as a multiphase system where different processes occur in each of the soil phases (e.g., Jury et al., 1984a, b, c; Baehr and Corapcioglu, 1987; Cohen and Ryan, 1989; Sleep and Sykes, 1989; Shoemaker et al., 1990; Gierke et al., 1990; Nair et al., 1990; Piver and Lindstrom, 1991a, b; Grifoll and Cohen, 1994). It has been demonstrated in various studies that water movement in the vadose soil zone can have a significant effect on contaminant volatilization from the soil (Jury et al., 1983, 1984a, b, c; Rosenbloom et al., 1993; Cohen and Ryan, 1989). The effect of water movement on contaminant transport is closely coupled with climatic variations (e.g., rainfall) and thus can affect contaminant transport in the vadose zone (Nofziger and Hornsby, 1986; Jury and Gruber, 1989; Russo et al., 1989a, b; Edwards et al., 1992; Oppong and Sagar, 1992; Haan et al., 1994). For example, the recent study of Haan et al. (1994), which considered stochastically generated dynamic rainfall and evapotranspiration conditions, coupled with a convection-only contaminant transport model, demonstrated that, due to the stochastic nature of rain, the use of an average or a single weather sequence can yield contaminant transport results that are far from the mean. Earlier studies on the coupling of climatic variability with contaminant transport in the unsaturated soil zone have focused on approaches that essentially assumed a time- and/or depth-invariant water velocity or moisture content (Haan et al., 1994; and references therein). It is worth noting, however, that the impact of transient water flow conditions (due to transient irrigation) and the ensuing variability of the water content profiles on the transport of a non-volatilizing solute in soils has been recognized in the work of Russo et al. (1989a, b). In these latter studies it was shown that under transient conditions, at any given time, portions of the soil may be wetting while other parts may be draining. The detailed account of the dynamic coupling between climatic variations (i.e. focusing on rainfall and evapotranspiration) and contaminant transport, and the significance of the various transport mechanisms (i.e. diffusion, dispersion and convection), as affected by the dynamic variation of moisture content with depth and time, has not been the focus of earlier studies. Noted exception is the work of Piver and Lindstrom (1991a, b) who discussed various numerical modeling techniques of handling the complexity of contaminant transport in the soil, as affected by the dynamics of rainfall, evapotranspiration and temperature variations.

Earlier studies have clearly demonstrated the potential significance of weather sequences and moisture movement, when describing contaminant movement in the soil matrix. Therefore, it seems reasonable to expect that the details of contaminant movement can only be revealed through a modeling approach which considers the dynamics of rainfall and evapotranspiration. Accordingly, the motivation of the present work is to illustrate, via a deterministic model, the effect of transient water movement (associated with rainfall and evapotranspiration) on contaminant volatilization. In the present approach, the movement of water in the soil matrix is simulated using Richards' (1931) equation with the appropriate self-consistent surface boundary conditions (for rainwater infiltration and evapotranspiration) during rainy and non-rainy periods. Also,

air movement which is generated in the soil matrix, as the consequence of displacement by water, is taken into account in the model formulation. The solute mass transfer equations are then solved to provide a detailed account of the chemical concentration profiles and the contribution of diffusion, dispersion and convection transport mechanisms to chemical migration through the soil.

2. Physical basis and governing equations

The present study of the impact of rainfall and evapotranspiration on contaminant transport in the vadose zone focuses on a deterministic, one-dimensional isothermal description of water and chemical transport. In the present analysis the soil hydraulic conductivity is taken to be a function of water content which in turn varies with depth. All other soil parameters such as the soil porosity, organic carbon content, percent clay and sand, and hydraulic conductivity at saturation are taken to be depth-invariant when solving the model equations. As a further simplification, the soil domain is considered to be isothermal. Admittedly, the above simplifications are too restrictive for site-specific field applications. In principle, heterogeneities, non-isothermal and non-equilibrium effects can be included via more complex modeling efforts. However, the simplified approach adopted here is sufficient for the current task which is to illustrate the effect of rain infiltration and evapotranspiration on contaminant transport.

2.1. Water movement

It is well established that soil water movement can be described by Richards' equation which for one-dimensional (i.e. vertical) transport can be written as (Bear, 1972):

$$\frac{\partial \theta_w}{\partial t} = -\frac{\partial}{\partial z}\left[-K\frac{\partial(\psi - z)}{\partial z}\right] \tag{1}$$

where θ_w is the soil water volume fraction; t is time; z is depth from the soil surface; K is the hydraulic conductivity; and ψ is the matric potential. K and ψ both depend on the volumetric water content of the soil and the soil type. In this study, the dependence of the matric potential and the hydraulic conductivity on the soil water content, is approximated by the following empirical relations (van Genuchten, 1980; see also Nielsen et al., 1986):

$$K = K_s\sqrt{\Theta}\left[1 - \left(1 - \Theta^{1/m}\right)^m\right]^2 \tag{2}$$

$$\psi = -\frac{1}{\alpha}\left(\frac{1}{\Theta^{1/m}} - 1\right)^{(1-m)} \tag{3}$$

where Θ is the dimensionless effective degree of water saturation defined as

$$\Theta = \frac{\theta_w - \theta_{wr}}{\epsilon - \theta_{wr}} \tag{4}$$

in which θ_{wr} is the residual water volume fraction; and ϵ is the soil porosity. K_s is the hydraulic conductivity at saturation and α and m are empirical soil-dependent parameters. The soil parameters in Eqs. 2–4 can be estimated using the correlations of Rawls and Brakensiek (1985), which provide θ_{wr}, α, m and K_s as functions of the percentage of clay and sand of the soil, and the soil porosity.

Eqs. 1–4 allow the simulation of water movement in soils subject to the appropriate boundary conditions are used. At the soil surface, i.e. $z = 0$, the water velocity can be set equal to rainfall infiltration velocity under the non-ponding condition and it is set equal to the saturated hydraulic conductivity when ponding condition is reached. During non-rainy periods water evaporation from the soil surface depends on the potential evapotranspiration and, according the Dalton law analogy (Bras, 1990), on the vapor pressure gradient. Accordingly, the volumetric water evapotranspiration flux can be expressed as:

$$J_e = \mathrm{PEV}\left(\frac{h_s - h_a}{1 - h_a}\right) \tag{5}$$

where h_a and h_s are the relative humidities in the air and in the soil surface, respectively; and PEV is the potential evapotranspiration (Bras, 1990), i.e. the evapotranspiration rate that would take place in the absence of water supply limitations at the air–soil interface. There are different approaches to evaluate PEV, and in the test cases presented in this study the simple Thornthwaite (1948) equation which requires average monthly temperatures was used. The relative humidity over the surface of the soil pore water, h_s, can be related to the matric potential at the soil surface, ψ_s, by (Edlefson and Anderson, 1943):

$$h_s = \exp\left[\frac{Mg\psi_s}{RT}\right] \tag{6}$$

where M is the molecular weight of water; g the gravitational acceleration; R is the universal gas constant; and T is temperature. Finally, at the bottom boundary, $z = L$, the condition of a zero matric potential gradient was used. This boundary condition is a reasonable approximation when the soil depth being considered is sufficiently large such that, for the duration of the simulation, there is negligible water migration at the bottom boundary.

2.2. Air movement

Air which is present in the interstices of the porous soil matrix is exchanged with the atmospheric air when the water content near the soil surface changes due to rain infiltration and evapotranspiration. Soil-gas phase movement can also be the result of natural convection such as due to temperature gradients (Cohen et al., 1988; Piver and Lindstrom, 1991a, b). However, these secondary effect are not considered in the present study. Assuming that the soil porosity, ϵ, is time-invariant and that $\epsilon = \theta_a + \theta_w$, where θ_a and θ_w are the volume fractions of the soil-air and soil-water, respectively, it then follows that:

$$\frac{\partial(\theta_a + \theta_w)}{\partial t} = 0 \tag{7}$$

and with the use of the continuity equation the following relation between the water and air convective fluxes is obtained

$$\frac{\partial(q_a + q_w)}{\partial z} = 0 \tag{8}$$

in which q_a and q_w are the Darcy's volumetric fluxes of air and water, respectively. In writing Eq. 8 it is assumed that the gas phase can be considered to be incompressible given the restriction of isothermal condition and that the total gas pressure is about atmospheric pressure.

The bottom boundary of the vadose zone can be taken to be impermeable to the air phase, i.e. $q_a = 0$ @ $z = L$. It is noted that this boundary condition and Eq. 8 cannot be used when the condition of ponding is reached. For this condition of ponding the above approach predicts that the air is entrapped, in the soil pore space, even though θ_a is changing near the soil surface. To overcome this limitation, the boundary condition at the soil surface, under the condition of ponding, can be changed to $q_a = 0$ @ $z = 0$. This latter boundary condition implies that, under the condition of ponding, atmospheric air does not penetrate the soil surface (i.e. @ $z = 0$).

It is emphasized that in the present analysis air movement is the result of either displacement by water or replacement of void space created by the water. There are other possible mechanisms for air movement such as due to natural convection near the surface region as the consequence of temperature gradients. Such secondary effects are worth exploring; however, this requires detailed temporal information on the coupled moisture and temperature–depth profiles in the soil (Cohen and Ryan, 1989). Such information on self-consistent moisture and temperature profiles can be obtained experimentally for specific location or simulated with an appropriate model of coupled heat and mass transfer as described in a detailed monograph by Piver and Lindstrom (1991a).

2.3. Pollutant transport

One-dimensional chemical transport in the multiphase soil matrix consisting of M phases, can be described by the following set of unsteady convection–diffusion equations:

$$\frac{\partial \theta_i C_i}{\partial t} = \frac{\partial}{\partial z}\left[\theta_i\left(\frac{D_i}{\tau_i} + D_{vi}\right)\frac{\partial C_i}{\partial z}\right] - \frac{\partial}{\partial z}(\theta_i V_i C_i) + \sum_{\substack{j=1 \\ j\neq i}}^{M} a_{ij} N_{ij} + R_i \theta_i$$

$$i, j = 1, \ldots, M \tag{9}$$

in which C_i and V_i are the chemical concentration and interstitial velocity for phase i, respectively; N_{ij} is the chemical mass flux from phase j to i; and a_{ij} is the interfacial area per unit volume of soil matrix between phases i and j. The chemical molecular mass diffusion and convective dispersion coefficients in phase i are denoted by D_i and D_{vi}, respectively, and the tortuosity of phase i is given by τ_i. Finally, the rate of chemical or biochemical transformations in phase i is given by R_i, where degradation of the chemical occurs when $R_i < 0$ and production occurs when $R_i > 0$.

The solution of the coupled set of individual mass transfer equations (see Eq. 9), for the three soil phases (soil, air and water), is required when the resistance to mass transfer among the soil phases is significant (Cohen and Ryan, 1989; Gierke et al., 1990; Imhoff and Jaffé, 1994). Mass transfer limitations are sensitive functions of the soil type, the physicochemical properties of the chemical (e.g., diffusivity, partition coefficients) and the flow conditions. In another recent study, Imhoff and Jaffé (1994) showed that mass transfer coefficients can vary significantly depending on the soil structure and uniformity of water flow in the soil. These authors also suggested that air–water mass transfer coefficient correlations, based on laboratory data, may not be representative of field conditions. Earlier studies by Cohen and Ryan (1989) and Gierke et al. (1990) suggested that the local equilibrium assumption for air–water mass transfer is reasonable for volatile chemicals. Mass transfer limitations for solute adsorption have also been documented in the literature and these are also known to depend on the soil structure and composition as well as on the degree of water saturation and water movement in the soil. Treatment of non-equilibrium processes while desirable is not the focus of the present work.

In the present analysis we retain the more restrictive local-equilibrium condition that has been commonly employed in the literature (Jury et al., 1983, 1984a, b, c, 1990; Nair et al., 1990; Shoemaker et al., 1990; Piver and Lindstrom, 1991a, b; Grifoll and Cohen, 1994). This simplification is believed to be sufficient for illustrating the potential impact of climatic variability and ranking its relative importance for different chemicals. Accordingly, subject to the restriction of local phase equilibrium, the mass transfer equations as expressed in Eq. 9, can be written in terms of the overall chemical concentration in the soil matrix:

$$\frac{\partial C_{sm}}{\partial t} = \frac{\partial}{\partial z}\left[D_{ap} \frac{\partial (C_{sm}/\xi)}{\partial z} - V_{eff} C_{sm} \right] + R_{sm} \tag{10}$$

where C_{sm} is the total soil matrix chemical concentration given by

$$C_{sm} = \frac{(\text{mass of polluant})}{(\text{unit soil volume})} = \theta_a C_a + \theta_w C_w + \theta_s C_s \tag{11}$$

and

$$\xi = \theta_a + \theta_w \frac{1}{H_{aw}} + \theta_s \frac{H_{sw}}{H_{aw}} \tag{12}$$

where the sub scripts s, w and a refer to the soil-solids, soil-water soil-air phases, respectively; and H_{ij} is the partition coefficient between soil phases i and j defined as:

$$H_{ij} = \frac{C_i}{C_j} \tag{13}$$

The effective convective velocity is denoted by V_{eff} and the apparent chemical diffusion coefficient, D_{ap}, in the soil matrix is given by:

$$D_{ap} = \theta_a \left(\frac{D_a}{\tau_a} + D_{va} \right) + \frac{\theta_w}{H_{aw}} \left(\frac{D_w}{\tau_w} + D_{vw} \right) \tag{14}$$

where it is noted that when the physicochemical properties of the soil are uniform with depth (i.e. when ξ is constant) the commonly defined effective soil diffusion coefficient (Jury et al., 1984c; Ryan and Cohen, 1990), D_{eff}, is given as $D_{\text{eff}} = D_{\text{ap}}/\xi$. In the present analysis the tortuosity factors, τ_{a} and τ_{w}, were evaluated according the model of Millington (1959), i.e. $\tau_i = \epsilon^2/\theta_i^{2.3}$. The longitudinal dispersion coefficient in each phase, D_{va} and D_{vw}, were estimated as $D_{\text{v}i} = \alpha_{\text{L}_i} V_i$ (Bear, 1972) where α_{L_i}, longitudinal dispersivity in phase i, has been evaluated by various authors for different levels of soil saturation levels. For example, Wierenga and van Genuchten (1989) evaluated the longitudinal dispersivity in a 6-m-long column to be ~ 5.5 cm, whereas Jaynes (1991) conducted a series of experiments in soil plots of varying depth and reported the longitudinal dispersivity to range from 4.5 to 28.8 cm. Butters and Jury (1989) have shown that the dispersivity varies with the solute travel distance; over a depth of ~ 4 m the dispersivity was reported to vary from ~ 5 to 30 cm. In earlier field experiments Biggar and Nielsen (1976) reported a longitudinal dispersivity value of $\alpha_{\text{L}} = 7.8$ cm for saturated soil conditions in an agricultural field. For unsaturated soils, conclusive field data for α_{L} are lacking but laboratory studies have shown that α_{L} increases when the soil volumetric water content decreases (van Genuchten and Wierenga, 1977; van Genuchten et al., 1977; Patel and Greaves, 1987). In the case study presented in this work, the variation of the longitudinal dispersion in the soil water and air phases, as a function of the volumetric phase saturation, $S_{\text{w}} = \theta_{\text{w}}/\epsilon$, was estimated based on the detailed numerical study of dispersion in porous media provided by Sahimi et al. (1986). Based on the results of the Sahimi et al. (1986), the following empirical correlations were developed:

$$\alpha_{\text{L}_i}(S_i) = \begin{cases} \alpha_{\text{L}_i}(1)\left[1 - 1.31(S_i - 1)\right]; & S_i > 0.53 \\ \alpha_{\text{L}_i}(1)\left[14.6 - 24.3S_i\right]; & S_i < 0.53 \end{cases} \tag{15}$$

where $\alpha_{\text{L}_i}(1)$ is the longitudinal dispersivity at $S_i = 1$. Eq. 15 predicts a dispersivity which is nearly constant, equal in value to the dispersivity at the saturation limit, until the volumetric content of phase i reaches 0.53. Below this characteristic value, the dispersivity increases sharply, with a theoretical limit of $14.6\alpha_{\text{L}_i}(1)$. It is important to note that the adoption of the above empirical longitudinal dispersivity model is not meant to suggest its general applicability. Clearly, contaminant transport in specific soils and specific environmental conditions will depend on the soil-specific longitudinal dispersivity and its variation with moisture content. Therefore, one may expect that the quantitative importance of dispersion, relative to other transport mechanisms, will depend on the soil-specific longitudinal dispersivity and its variation with moisture content. Nonetheless, the relation selected in the present case study suffices given that we merely use Eq. 15 to demonstrate a possible set of transport behavior.

The effective convective velocity, V_{eff} in Eq. 16, is defined as:

$$V_{\text{eff}} = \frac{1}{\xi}\left(\theta_{\text{a}} V_{\text{a}} + \frac{\theta_{\text{w}} V_{\text{w}}}{H_{\text{aw}}}\right) \tag{16}$$

where V_{a} and V_{w} are the interstitial velocities in the soil-air and soil-water phases,

respectively; and ξ is defined in Eq. 12. The water phase interstitial velocity is obtained from:

$$V_w = -\frac{K}{\theta_w}\left(\frac{\partial \psi}{\partial z} - z\right) \tag{17}$$

and the air phase velocity was obtained using Eq. 8.

Finally, the overall reaction rate, i.e.:

$$R_{sm} = \sum_{i=1}^{M} R_i \theta_i$$

which accounts for bio- and chemical transformations, depends (in addition to on the chemical concentration) on the specific soil characteristics and its microorganism community (Lyman et al., 1990; Howard et al., 1991; Mackay et al., 1992). Therefore, it is generally not possible to utilize a single set of representative reaction rate constants for a given transformation process. Thus, in the present study, we focus on elucidating the relative importance of the various transport mechanisms in the absence of reactions. However, a limited number of simulations included degradation carried out as discussed later.

The evolution of the concentration profiles is obtained by solving Eq. 10, given V_{eff}, D_{ap} and ξ as a function of time and depth, and subject to the appropriate initial and boundary conditions. In this work the volatilization boundary condition was set at the soil–atmosphere interface. Accordingly, the chemical surface volatilization flux, J_0, is given by:

$$J_0 = k_{atm}(C_{atm} - C_a) \ @ \ z = 0 \tag{18}$$

where k_{atm} is the atmospheric-side mass transfer coefficient between soil and atmosphere, which can be evaluated, for instance, by the semi-empirical correlation proposed by Brutsaert (1975); and C_{atm} is the bulk pollutant concentration in the atmospheric phase (see also Grifoll and Cohen, 1994). In all the simulations the depth of the soil was selected to be sufficiently large to ensure that the chemical concentration front (i.e. non-zero concentration values) did not reach the bottom boundary over the length of the simulation. Therefore, the bottom boundary can be conveniently set as either $C_{sm} = 0$ @ $z = L$ or $\partial C_{sm}/\partial z = 0$ @ $z = L$. The use of either of these boundary conditions yields essentially identical results so long as the restriction of a large depth, relative to the downward movement of the concentration front, is met. We note that in a more general approach a non-zero flux boundary condition is particularly useful when it desired to interface the vadose zone model with a groundwater contaminant transport model.

2.4. Numerical solution scheme

The one-dimensional transport equations for moisture (Eq. 1) and chemical pollutant (Eq. 10) were solved by an implicit finite-difference approach. Eq. 1 was first transformed by applying a hyperbolic sine transform to the matric potential following the

method of Ross (1990). Accordingly, the following new independent variable was defined:

$$p = \begin{cases} \sinh^{-1}\left(-\dfrac{\psi - \psi_0}{\psi_1}\right); & \psi < \psi_0 \\ -\dfrac{\psi - \psi_0}{\psi_1}; & \psi > \psi_0 \end{cases} \tag{19}$$

The transformed Eq. 1 and Eq. 10 were discretized using a fully implicit scheme with a central differencing for the second derivatives and backwards differencing for the first derivative (Fletcher, 1991). The discretized model equations for water movement were solved using the Newton–Raphson iteration procedure. For the range of simulation conducted in the present study, the soil domain was divided into three zones. The first zone from $z = 0$ to $z = z_1$ with a constant step size equal to Δz_1, a second zone from $z = z_1$ to $z = z_2$ with increasing step size such that $\Delta z_i = r_1 \Delta z_{i-1}$, and a third zone from $z = z_2$ to $z = L$ with a constant step size equal to Δz_2. Since steep concentration gradients normally occur in the surface region (i.e. near $z = 0$) a step size of $\Delta z_1 = 10^{-4}$ m was used from $z = 0$ to $z = 0.05$ m. In the second zone (0.05 m $< z <$ 0.81 m) r_1 was set to 1.05. Finally, in the third zone (0.81 m $\leq z \leq L$) the step size was set to $\Delta z_2 = 0.015$ m. A variable time step was selected between a minimum of 0.005 h and a maximum of 5 h to ensure that the solution was tracked along small incremental changes of the independent variable, p. This procedure was found to allow an accurate determination of the derivative $\partial p/\partial z$ which was used for the subsequent calculations of the water convective velocity. The numerical algorithm for the solution of Eq. 1 was checked against the analytical solution given by Broadbridge and White (1988) for the case of constant rainfall for a Brindabella silt clay loam soil. A comparison of the numerical and analytical solution is given in Fig. 1; it is observed that the numerical solution closely follows the analytical results. Most importantly, the numerical and analytical solutions are in excellent agreement near the soil surface, where the volatilization flux is most affected by the soil moisture and concentration profiles. It is important to note that, unlike the analytical solution, the numerical solution can handle time-variable boundary conditions and also deal with both ponding and non-ponding conditions.

The chemical transport model (Eq. 10) was solved with water and air interstitial velocities, evaluated from Eqs. 1 and 8, using a frilly implicit scheme (Fletcher, 1991). The resulting discretized algebraic system was a linear with tridiagonal-coefficient matrix and solved by the Thomas algorithm (Press et al., 1989). Finally, the grid size for both Eqs. 1 and 10 was set to minimize discretization errors and to comply with the restriction of, $N_{\mathrm{Pec}} = \Delta z V_{\mathrm{eff}}/D_{\mathrm{eff}} \ll 2$, for all grid cells, where N_{Pec} is the local grid cell Péclet number, thus ensuring that numerical dispersion effects were negligible (Fletcher, 1991; Piver and Lindstrom, 1991a).

3. Simulation set up

In order to illustrate the effect of rainfall dynamics and evapotranspiration on pollutant transport in the vadose zone a test case was synthesized for a hypothetical

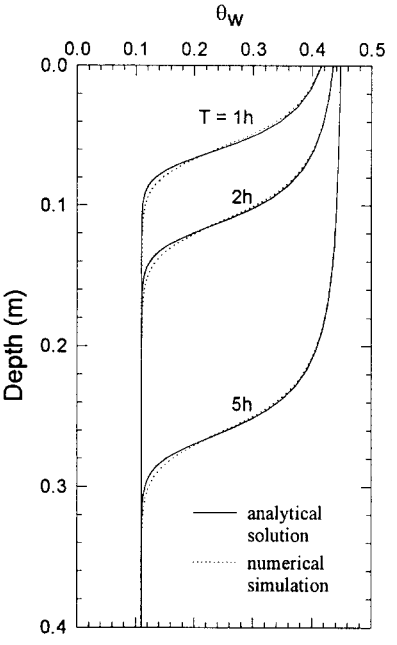

Fig. 1. Soil-water content profiles for a constant rainfall of 1.65 cm/h. Comparison of the numerical solution of Eq. 1 to the analytical solution of Broadbridge and White (1988) for a clay–loam soil.

region of weather characteristics, that to some extent resemble the climate in Southern California. The soil selected for this test case was a loam-type soil with the characteristics given in Table 1. The soil hydraulic parameters required in Eqs. 2–4 were estimated from the empirical correlations of Rawls and Brakensiek (1985) with the corresponding

Table 1
Soil characteristics

Percent clay	10
Percent silt	30
Percent sand	60
Porosity, ϵ,	0.35
Organic carbon fraction	0.02

Table 2
Hydrological parameters (parameters required in Eqs. 2–4)

m	0.3
$1/\alpha$ (m)	0.233
θ_{wr}	0.022
K_s (m/s)	2.08×10^{-6}

Table 3
Rainfall and meteorological data set

	Temperature (°C)	Relative humidity	Precipitation (cm)	Wind speed (m/s)
Jan.	19.2	0.58	9.37	3.0
Feb.	20.3	0.62	7.52	3.1
Mar.	20.4	0.62	5.97	3.1
Apr.	21.6	0.65	2.97	2.9
May	22.9	0.67	0.58	2.8
Jun.	25.5	0.7	0.08	2.6
Jul.	28.8	0.68	0	2.4
Aug.	28.9	0.68	0.3	2.4
Sep.	28.3	0.65	0.53	2.6
Oct.	25.8	0.65	0.53	2.6
Nov.	22.6	0.54	4.7	2.9
Dec.	20.1	0.55	5.0	3.0

parameters listed in Table 2. A set of rainfall sequences, over a period of a year, was synthesized by selecting the pattern of monthly total rainfall shown in Table 3. This rainfall pattern was selected to approximately mimic the distribution of total monthly rainfall in southern California, U.S.A. (Ruffner and Bair, 1987). Single rainfall events

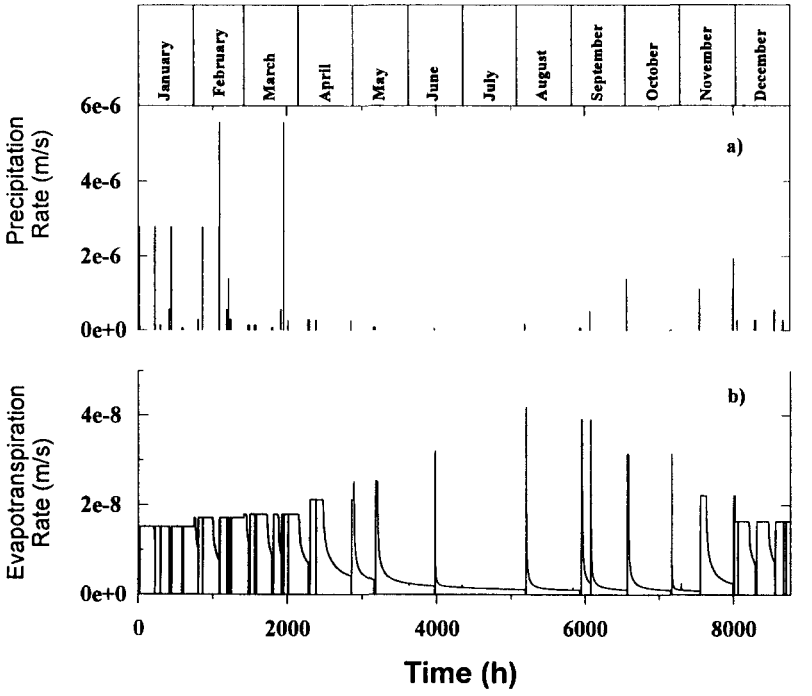

Fig. 2. (a) Precipitation rates and (b) evapotranspiration rates data set for the case study.

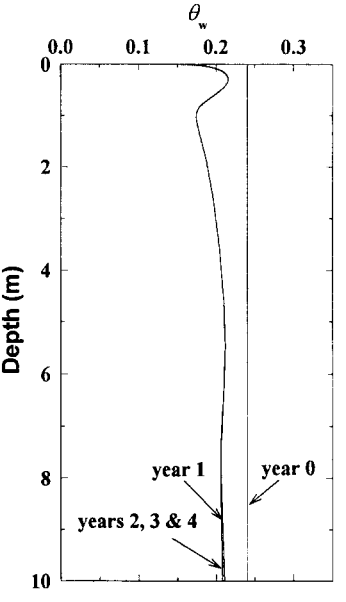

Fig. 3. Water content profiles on January 1 of year 1, initial condition, and successive years.

were then generated randomly, within each month, while maintaining the total rainfall for each month (see Fig. 2a). Monthly potential evapotranspiration (PEV) data, relative humidity in the air, average monthly temperatures, and wind speed data were selected from a consistent data set for the Los Angeles region as shown in Table 3. This selection was made simply in order to have a set of parameters which is reasonably consistent with the seasonal rainfall distribution given in Table 3. We note that in the present test case, evapotranspiration was allowed to occur only during non-rainy periods. The rate of evapotranspiration was determined from the solution of Eq. 1 in which the evapotranspiration boundary condition as given in Eq. 5 was used. The resulting distribution of evapotranspiration fluxes is shown in Fig. 2b.

The rainfall distribution (Fig. 2b) was first applied to a four-year simulation of moisture movement in the soil with a uniform initial moisture distribution (designated as year 0 in Fig. 3). This was done in order to arrive at a consistent yearly cycle of moisture variations. In order to initialize the simulation, the initial moisture value was chosen by setting the gravitational infiltration rate $[q_w = K(\theta_w)]$ equal to the year-average rainfall rate. After the fourth year of simulation, the moisture profiles evolved to a year-cyclic state where the moisture profile for any specific time during the fourth year was equivalent to the moisture profile at the same time in subsequent years. Thus, in the chemical transport simulations the moisture profiles in the soil, as a function of depth and time, were obtained from the corresponding moisture profiles for the fourth year moisture simulation results. Samples of the soil moisture profiles obtained for the fourth year are shown in Fig. 4. All of these profiles show, as expected, that during non-rainy periods there is a decrease of moisture content near the soil surface due to evapotranspi-

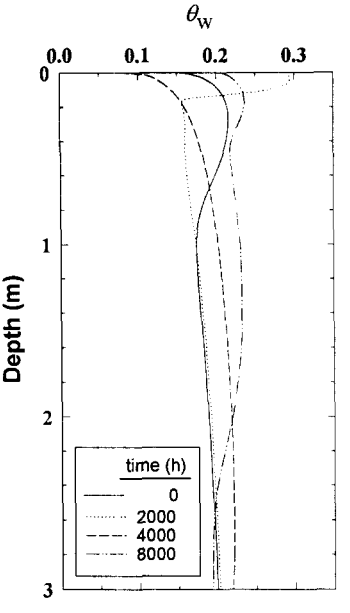

Fig. 4. Water content profiles at different times for the reference year used for the chemical transport case study.

ration. These moisture profiles are also irregular in shape due to the variability of the rain events and evapotranspiration.

The resulting moisture profiles and the corresponding water velocities, which were obtained throughout the fourth year, were used to evaluate the effective convective velocity, Eq. 16, and the dispersion coefficients (i.e. D_{vi}). Also, the apparent diffusion coefficient, D_{ap} (Eq. 14) and the parameter ξ (Eq. 12) were determined, as a function of moisture content, given the calculated moisture variation with depth and time. Instead of evaluating chemical transport for an arbitrary selection of physicochemical parameters the simulations were carried out for three chemicals: benzene, methanol and TCA. These chemicals were selected to provide a self-consistent set of physicochemical parameters that span a reasonable range of three orders of magnitude for the Henry's law constant. Benzene and TCA were selected as examples of volatile hydrophobic organics. Methanol was selected to demonstrate the behavior of a volatile water-soluble organic with negligible propensity to adsorb onto the soil solids. The pertinent physicochemical properties at 20°C for these substances are given in Table 4.

4. Results and discussion

The simulations were carried out for two different initial contamination scenarios. The initial soil matrix concentration condition, at the beginning of the simulation, was set either on January 1st or July 2nd. In all cases, the initial contamination was restricted

Table 4
Physicochemical properties for benzene, 1,1,2,2-tetrachloroethane (TCA) and methanol

	Benzene	TCA	Methanol
Molecular diffusion in air, D_a (m^2/s)[a]	0.88×10^{-5}	0.72×10^{-5}	1.6×10^{-5}
Molecular diffusion in water, D_w (m^2/s)[b]	0.90×10^{-9}	0.76×10^{-9}	1.4×10^{-9}
Aqueous solubility (g/l)[c]	1.78	2.9	soluble
Dimensionless Henry's law constant, H_{aw}	0.18[d]	1.92×10^{-2}[f]	1.9×10^{-4}[e]
Solid/water partition coefficient, H_{aw}^{g}[i]	1.5	2.5	1.80×10^{-3}
Organic carbon/water partition coefficient, K_{oc}	59[g]	100[h]	0.07[h]
Octanol-water partition coefficient, K_{ow}	132[g]	245[f]	0.17[e]

[a] Using the correlation of Fuller et al. (1966).
[b] Using the correlation of Hayduk et al. (1982).
[c] Mackay et al. (1992).
[d] Data from Leighton and Calo (1981).
[e] SRC CHEMFATE database.
[f] Howard (1987).
[g] Mackay et al. (1992). Average value reported by Olson and Davis (1990).
[h] Karickhoff (1981), $K_{oc} = 0.41\ K_{ow}$.
[i] Note: $H_{sw} = K_{oc} f_{oc} \rho_{bulk}$; $f_{oc} = 0.02$; $\rho_{bulk} = 1.27$ g/cm^3.

to the case of residual contamination (i.e. no free-phase of the contaminant present in the soil).

The soil matrix chemical concentration profiles, based on the simulation results obtained at $t = 0$, 500, 2000, 4000 and 8760 h, are depicted in Fig. 5 for the case of a soil initially contaminated down to a depth of ~0.5 m. It is apparent that the concentration profile for benzene is spread out more so than for TCA and methanol. The

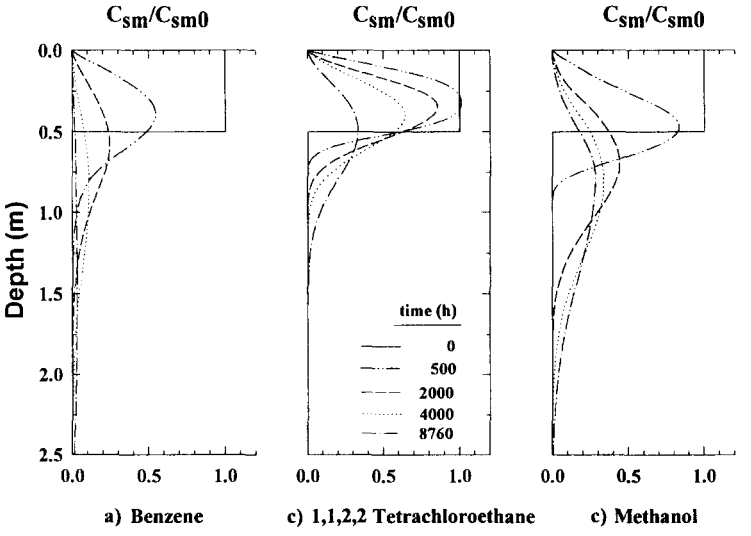

Fig. 5. Dimensionless concentration profiles for each chemical at $t = 0$, 500, 2000, 4000 and 8760 h: (a) benzene; (b) 1,1,2,2-trichloroethane; and (c) methanol. $t = 0$ denotes the beginning of the simulation on January 1st.

Table 5
Percent chemical mass distribution, at equilibrium, for a soil with 20% soil-air, 15% soil-water and 65% soil-solids

	Benzene	TCA	Methanol
Soil-air (20%)	3.10	0.22	0.03
Soil-water (15%)	12.92	8.43	99.20
Soil-solids (65%)	83.98	91.35	0.77

above behavior is consistent with the physicochemical properties for these chemicals and it can be easily understood by considering the case of chemical equilibrium partitioning among the three soil phases. As an example, the partitioning for a soil of porosity 0.35 and volumetric soil moisture content of 0.15 given in Table 5. Benzene, which partitions to the air phase, to a larger degree than TCA and methanol (see Table 5), is expected to diffuse mostly through the air phase when the relative water saturation is below ~ 0.9 (Grifoll and Cohen, 1994). This latter condition is prevalent during most of the simulation period and thus, the rapid diffusion of benzene through the air phase leads to a faster spreading of this chemical through the soil. In contrast, the air/water partition coefficient of TCA is much lower than that of benzene (see Table 4) while at the same time its adsorption coefficient (i.e. H_{sw}) is higher than that of both benzene and methanol. TCA partitions mostly to the soil solids (see Table 5) and thus its migration is retarded, relative to benzene and methanol, resulting in relatively greater persistence of TCA in the soil. During the time period extending from January 1 through the third quarter of March (i.e. the rainy period) chemical transport due to water convection (due to the infiltration of rainwater) is expected to be a significant chemical transport mechanism. Indeed, methanol which has the lowest air/water partition and soil/water partition coefficients, is expected to reside mostly in the soil-water phase (see Table 5) during the rainy season. Thus, methanol is expected to migrate deeper into the soil column relative to both benzene and TCA, due to rainwater infiltration, as discussed later in this section.

In order to assess the effect of water infiltration on chemical migration, simulations results for the full-rainfall case were compared to simulations for the case of a uniform and depth-invariant moisture content which was set equal to the yearly average moisture content. The results obtained for the three chemicals are shown in Fig. 6a–c in terms of the ratio of the chemical fluxes obtained with and without the consideration of the effects of water movement. It is evident that there are significant fluctuations of the volatilization flux throughout the 1-year simulation period. When most of the chemical is near the soil surface (i.e. near the beginning of the simulation), rain first promotes volatilization due to displacement of the near surface soil-air, which is rich in the chemical. As illustrated later in this section, near the surface region, where the concentration gradients are steep (and of a negative sign) dispersion of the chemical in the soil-water further enhances the volatilization flux. The enhancement of the volatilization flux is less pronounced as time progresses in the simulation since the chemical concentration decreases in the near-surface region and the concentration gradient at the soil surface gradually vanishes. Immediately, after the cessation of rainfall, the content

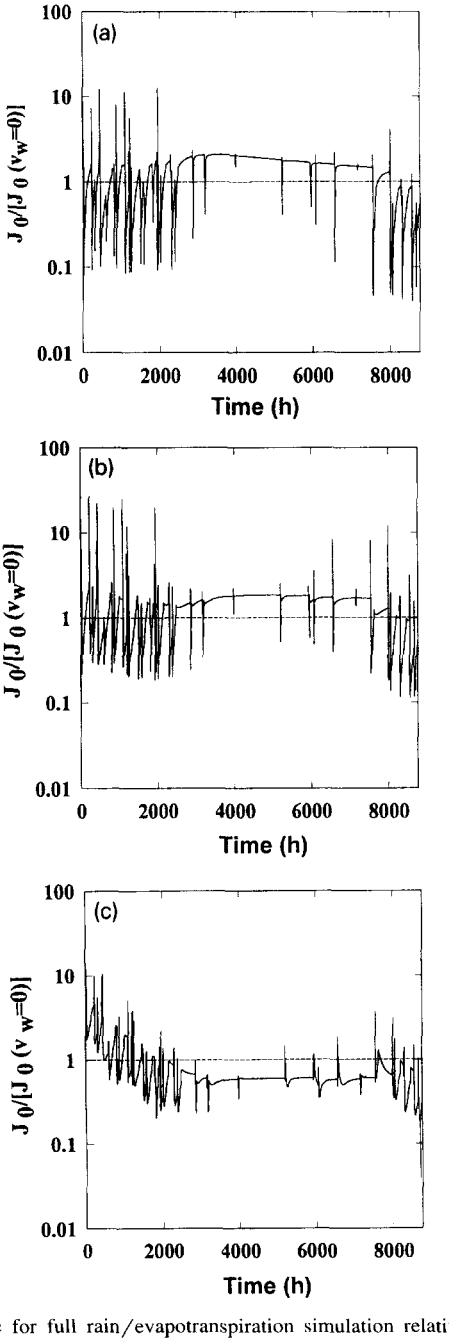

Fig. 6. The volatilization rate for full rain/evapotranspiration simulation relative to the case of no water movement for: (a) benzene; (b) *1,1,2,2*-trichloroethane; and (c) methanol. Initial contamination at $t = 0$ on January 1st.

of water in the surface soil region decreases due to water evapotranspiration and water infiltration (mainly by gravity flow). As a consequence of continuity, atmospheric air flows into the soil to occupy the void space freed by the soil-water thus retarding the rate of chemical volatilization from the soil. When most of the chemical is present deeper in the soil the above near-soil surface phenomenon is less important.

During the relatively non-rainy period (about mid-March to September; see Fig. 2a), the volatilization flux for benzene and TCA for most of this period is above the flux predicted in the absence of water movement. A detailed examination of the moisture profiles revealed that the full simulation analysis (i.e. where evapotranspiration and water infiltration are considered) results in moisture content, near the surface region, which is significantly lower than the year-average moisture content. Consequently, for the present weather scenario, the assumption of a constant and uniform moisture content (i.e. no-water movement scenario) leads to an underestimate of the effective chemical mass diffusivity (i.e. D_{ap}/ξ near the surface region). In contrast with the above results, it is interesting to note that, for methanol, during the same period (about mid-March to September; see Fig. 2a), the volatilization flux is in general (i.e. except for short durations during a few rain periods) below the flux predicted in the absence of water movement (Fig. 6c). This behavior is due to the fact that methanol which is soluble in water is driven downward into the soil column during rainy periods to a greater extent than benzene and TCA. Consequently, methanol volatilizes at a lower rate than would be predicted for the case of a constant moisture content (i.e. where methanol does not penetrate as deep into the soil). The effect of water movement due to both rainwater infiltration and evapotranspiration, as depicted in Fig. 6a–c, can be also quantified in terms of the average volatilization flux. For benzene, TCA and methanol the year-average volatilization flux, under the influence of rainfall and evapotranspiration, is higher by $\sim 6.1\%$, $\sim 38\%$ and $\sim 41.4\%$, respectively, relative to the no-water movement case.

Prior to discussing the relative importance of the various transport mechanisms (i.e. diffusion, dispersion and convection), it is instructive to illustrate the concentration and water moisture profiles, at a time near the occurrence of specific rainfall events. Methanol was selected for this example since methanol is most impacted by water movement. As shown in Fig. 7 the three-dimensional plot is shown of the moisture profile during the simulation segment from $t = 400$ h to $t = 500$ h (i.e. January 16 through January 20) with rain events of intensity of 0.2 mm/h, 0.1 mm/h and 1 cm/h occurring during the periods $t = 413$–423 h, $t = 423$–443 h and $t = 443$–445 h, respectively. Upon the initiation of the first rain event the moisture content and methanol concentration increase near the surface as seen in Figs. 7 and 8, respectively. Another significant rise in the water content near the surface and deeper in the soil is observed upon the initiation of the third rain event. As the rain continues, the chemical concentration deeper in the soil rises with a marked increase due to the third rain event (see Figs. 7 and 8). Clearly, methanol is driven deeper into the soil as the consequence of water infiltration.

The role of the different transport mechanisms in affecting contaminant movement through the soil, can be illustrated by inspecting the individual partial fluxes due to diffusion, dispersion and convection. The partial fluxes can be defined for each of the soil phases as given below

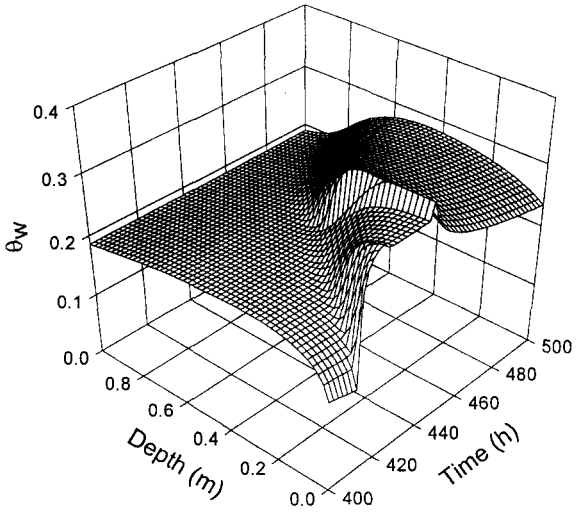

Fig. 7. Soil-water content as impacted by a series of rain events during the period $t = 400$–500 h.

diffusive flux:

$$J_{\mathrm{Dif}} = -\frac{\theta_i}{H_{ai}}\frac{D_i}{\tau_i}\frac{\partial(C_{\mathrm{sm}}/\xi)}{\partial z} \tag{20}$$

dispersive flux:

$$J_{\mathrm{Disp}} = -\frac{\theta_i}{H_{ai}}D_{vi}\frac{\partial(C_{\mathrm{sm}}/\xi)}{\partial z} \tag{21}$$

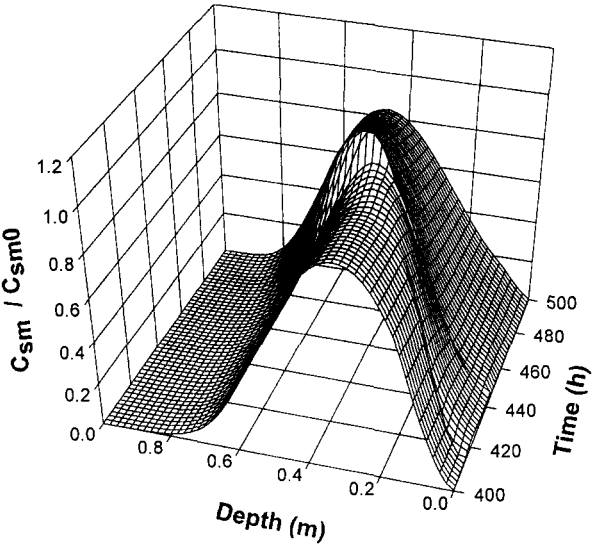

Fig. 8. Three-dimensional plot of the concentration profile for methanol corresponding the time period and soil-water content conditions depicted in Fig. 7.

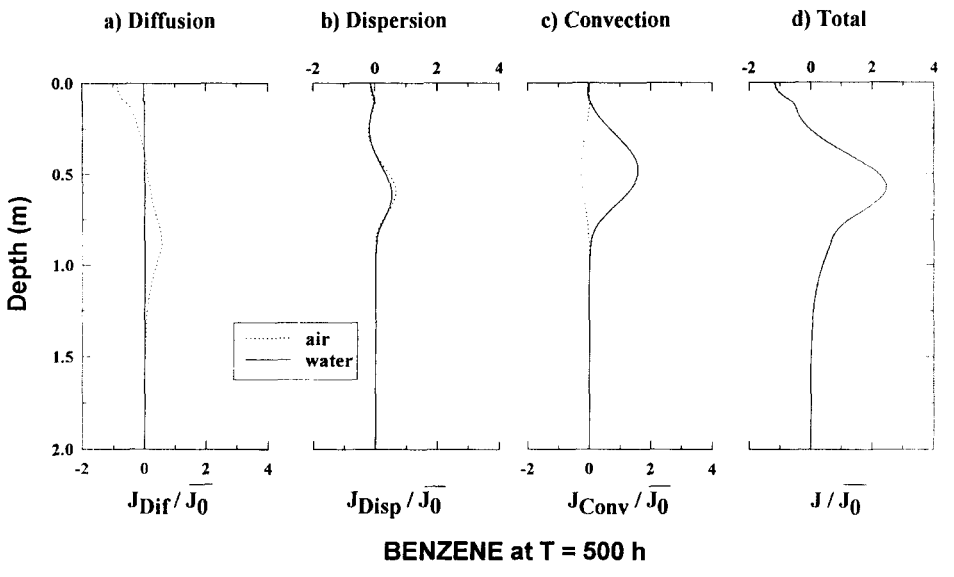

Fig. 9. Dimensionless chemical flux profiles for benzene at $t = 500$ h in the air and water phases due to: (a) diffusion; (b) dispersion; (c) convection; and (d) the total flux. Initial contamination on January 1st.

Convective flux:

$$J_{\mathrm{Conv}} = \frac{\theta_i}{H_{ai}} v_i \frac{C_{\mathrm{sm}}}{\xi} \tag{22}$$

The above partial fluxes, non-dimensionalized with respect to the year-average volatilization flux are given in Figs. 9–14 for two different simulation scenarios, respectively. In the first scenario the chemicals were initially placed in the soil on January 1st, just past midnight (i.e. $t = 0$ as indicated in Fig. 2b and 4). In the second scenario the chemicals were placed in the soil on July 2nd at noon, i.e. in the middle of the year. The first and second scenarios will be referred to hereinafter as January and July contamination scenarios, respectively. These two scenarios were selected to demonstrate chemical transport during: (a) a time period during the rainy season which follows a series of rain events (January contamination scenario); and (b) a time period during the non-rainy period (July contamination scenario). These scenarios were also selected to illustrate that the time period in which the contaminant is released can significantly affect the evolution of the concentration–time profiles and thus the half-life of the chemical in the soil. In both scenarios, simulation results for the partial fluxes are shown at a time of 500 h after the initial placing of the contaminants.

The results for the January contamination scenario reveal that transport via diffusion is significant only for benzene (Fig. 9). Benzene is present in the soil down to a depth of ~ 1.54 m with a maximum in the benzene partial diffusion flux, J_{dif}, at $z = 0.86$ m, where the air phase chemical concentration has its steepest gradient. In contrast, for TCA (Fig. 10) diffusive transport is apparent only in the top soil layer (down to ~ 0.7

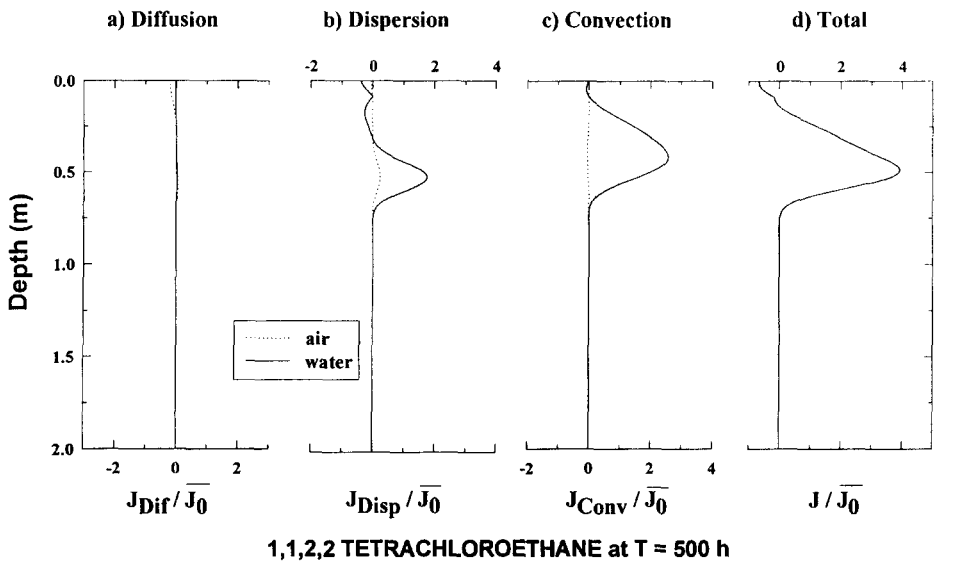

Fig. 10. Dimensionless chemical flux profiles for *1,1,2,2*-trichloroethane at $t = 500$ h in the air and water phases due to: (a) diffusion; (b) dispersion; (c) convection; and (d) the total flux. Initial contamination on January 1st.

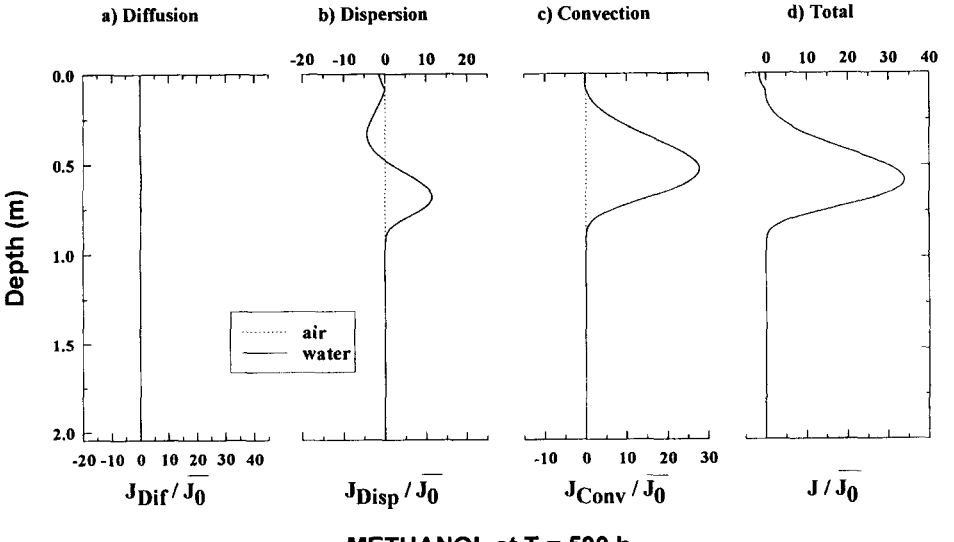

Fig. 11. Dimensionless chemical flux profiles for methanol at $t = 500$ h in the air and water phases due to: (a) diffusion; (b) dispersion; (c) convection; and (d) the total flux. Initial contamination on January 1st.

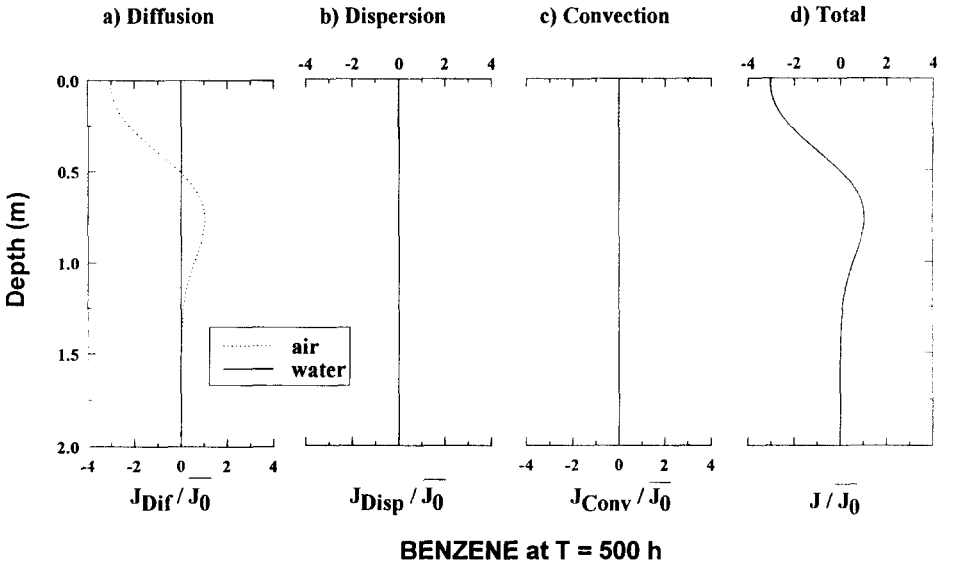

Fig. 12. Dimensionless chemical flux profiles for benzene at $t = 500$ h in the air and water phases due to (a) diffusion, (b) dispersion, (c) convection and (d) the total flux. Initial contamination on July 2nd.

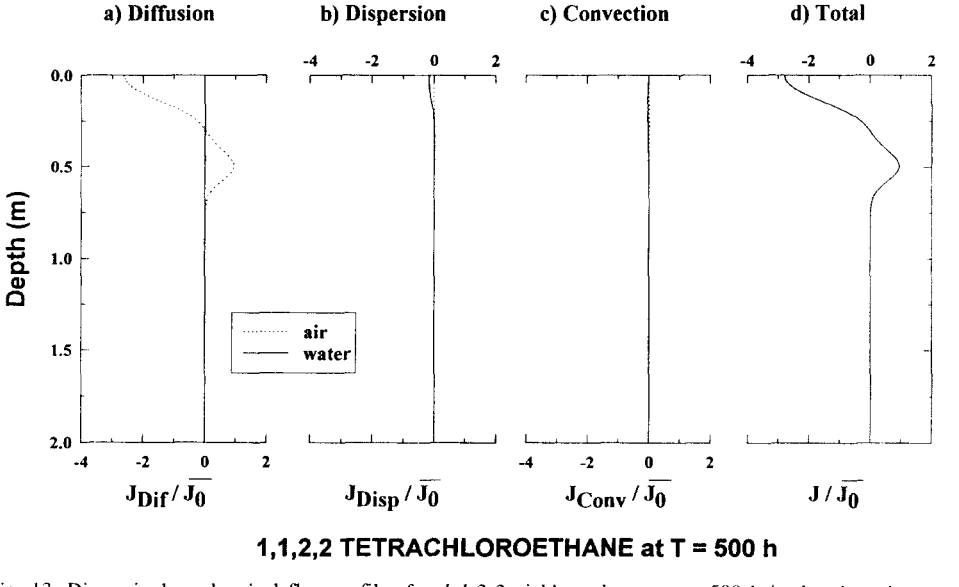

Fig. 13. Dimensionless chemical flux profiles for *1,1,2,2*-trichloroethane at $t = 500$ h in the air and water phases due to: (a) diffusion; (b) dispersion; (c) convection; and (d) the total flux. Initial contamination on July 2nd.

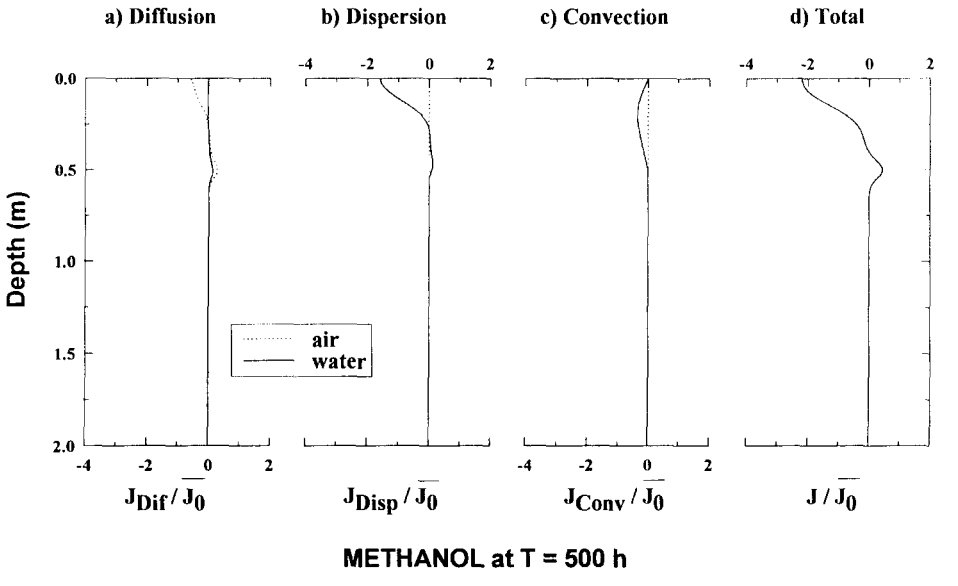

Fig. 14. Dimensionless chemical flux profiles for methanol at $t = 500$ h in the air and water phases due to: (a) diffusion; (b) dispersion; (c) convection; and d) the total flux. Initial contamination on July 2nd.

m below the surface) while for methanol diffusive transport is negligible (Fig. 11). Chemical transport by dispersion is important for all three chemicals. For benzene dispersive transport via the air and water phases is of a similar magnitude. Benzene movement occurs both downward and upward where the depth of ~ 0.38 m marks the transition point (Fig. 9). As expected from the dependence of the dispersive flux on the air/water partition coefficient (Eq. 21), TCA and methanol which have much lower air/water partition coefficients relative to benzene, demonstrate a much higher dispersive flux (both upward and downward) via the water phase. It is interesting to note that, very near the surface, the contribution of dispersion to the volatilization flux of the three chemicals is significant. Near the surface, the concentration gradient is steep and of a negative sign (i.e. increasing concentration with depth); thus, water movement results in a dispersive flux which enhances the chemical volatilization flux. Over most of the contamination zone, convective transport via the water phase is primarily downwards; an exception is the region in the immediate vicinity of the surface where water movement upward (due to evapotranspiration) enhances the volatilization flux.

The results for the July contamination scenario (i.e. during the relatively non-rainy period) reveal a strikingly different pattern (Figs. 12–14). The transport of both benzene and TCA is dominated by diffusion through the air phase (Figs. 12 and 13, respectively). This is not surprising given that, even with a high soil water content, these chemicals with a high air/water partition coefficients chemicals will migrate largely through the air phase (Grifoll and Cohen, 1994). For TCA, however, there is a slight contribution of both convective and dispersive fluxes by the water phase to the volatilization flux. This behavior is expected since the concentration gradients for TCA are much steeper than

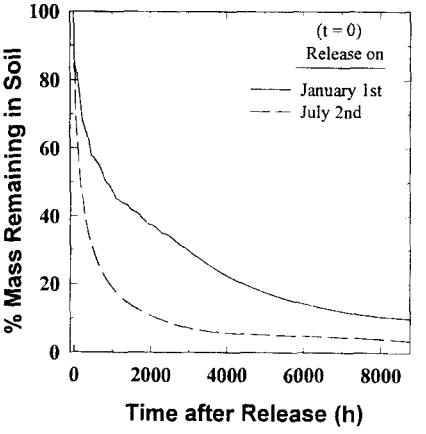

Fig. 15. Percent benzene remaining in the soil after initial contamination on January 1st and on July 2nd for benzene.

for benzene for the same time period. Finally, we note that the transport of methanol, which has the lowest air/water partition coefficient among the three test chemicals, is dominated by dispersion and convection. It is noted, however, that for methanol diffusive transport near the surface is also important (Fig. 14). This result and the result for the January contamination scenario (Fig. 11) suggest that, for chemicals with a low air/water partition coefficient convective and dispersive transport due to water movement can be significant during both rainy and non-rainy period so long as there is moisture movement in the soil. It should be noted that, with the exception of dry soil conditions, non-uniform soil moisture profiles which would lead to convective and dispersive transport should be expected under most field conditions.

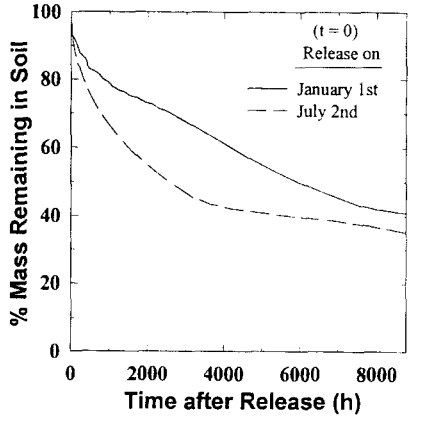

Fig. 16. Percent *1,1,2,2*-trichloroethane remaining in the soil after initial contamination on January 1st and on July 2nd for *1,1,2,2*-trichloroethane.

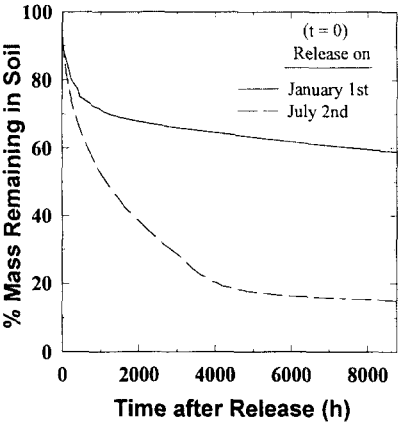

Fig. 17. Percent methanol remaining in the soil after initial contamination on January 1st and on July 2nd.

Another instructive illustration of the impact of the time of initial contamination on the percent of the chemical remaining in the soil is depicted in Figs. 15–17. In all cases, the rate of disappearance of the contaminant from the soil is much faster when the initial contamination is in July rather than in January. As, reasoned previously, during the rainy season, convection and dispersion lead to a greater spreading of the chemical. As a result, lower local concentrations and concentration gradients result in a lower volatilization flux from the soil via the three different transport mechanisms. As seen from a comparison of Figs. 15 and 16, the rate of disappearance of TCA (Fig. 16), for both contamination scenarios, is lower than for benzene. This behavior is consistent with the lower air/water partitioning and greater adsorption coefficient of TCA. Finally, most striking is the comparison of the January and July scenarios for methanol (Fig. 17). Methanol is most impacted by water movement in the soil and thus, for the January contamination scenario, there is a rapid decline in the rate of volatilization relative to the July scenario. Clearly, methanol which contaminates the soil during the rainy season will persist to a significantly greater extent than methanol which contaminates the soil during the non-rainy season.

While the above results and corresponding discussion pertains to conditions for which degradation is negligible, over the time scale of the simulation, it is worth commenting on the impact of degradation. For example, simulations in which a relatively high chemical degradation half-life of 5 days was used revealed that the difference between the percent of the chemical which volatilized for the complete water movement simulation relative to the no-water movement simulations was small (less than a few percent). When degradation is sufficiently rapid water movement has a diminishing impact on the chemical volatilization rate. From the present test cases (including simulations with chemical degradation) it can be concluded that the importance of water movement will increase as the air–water partition coefficient decreases and as the chemical propensity to degrade in the soil diminishes.

Finally, although the current simulations were with an initial contamination zone extending from the surface downward, it is worth noting that the present analysis can be

easily extended to accommodate other scenarios. One would expect that the volatilization flux will be lower when the initial chemical contamination zone is deeper into the soil. However, as the chemical is placed deeper into the soil, the impact of water movement on volatilization will be less noticeable.

5. Conclusions

Contaminant transport in the unsaturated soil zone, under the influence of the dynamics of rainfall and evapotranspiration was investigated using a deterministic numerical model. In order to illustrate the effect of water movement in the soil on the operating chemical transport mechanisms test cases for a loam-type soil and a synthesized data set of weather characteristics were used. Chemical transport simulations were carried out for of benzene, *1,1,2,2*-trichloroethane and methanol. The model simulations revealed that, at different times during the year long simulation, convection, dispersion and diffusion transport mechanisms contributed to different levels to the flux of the contaminant upward and downward the soil column. The present study suggests that an accurate description of contaminant transport, for periods during which there is a significant variation in rainfall and evapotranspiration, requires careful consideration of all the chemical transport mechanisms and the temporal variations in moisture profiles. Moreover, it was shown that the average volatilization flux, calculated based on year-average conditions, can deviate significantly (from $\sim 6\%$ to $\sim 40\%$ for the present test cases) from the average flux obtained when the dynamics of water movement in the soil is considered. This deviation is expected to be most important for chemicals with a low Henry's law constant and with a low propensity to degrade in the soil environment. Finally, it is stressed that the above findings are based on a specific soil transport model. Current work is ongoing to map out the effect of climatic variability on solute volatilization, for a variety of soil conditions, in which the simplifications used in the present analysis are relaxed (e.g., isothermal conditions, local-equilibrium and absence of immobile water phase).

Acknowledgements

This work was supported, in part, by the University of California Toxic Substances Research and Training Program. Also, the financial assistance received from the DGICYT of Spain, project No. PB92-0742, is gratefully acknowledged.

References

Baehr, A.L. and Corapcioglu, M.Y., 1987. A compositional multiphase model for groundwater contamination by petroleum products, 2. Numerical solution. Water Resour. Res, 23(1): 2101–213.

Bear, J., 1972. Dynamics of Fluids in Porous Media. American Elsevier, New York, NY.

Biggar, J.W. and Nielsen, D.R., 1976. Spatial variability of the leaching characteristics of a field Soil. Water Resour. Res., 12(1): 78–84.

Bras, R.L., 1990. Hydrology. Addison-Wesley, Reading.

Broadbridge, P. and White, I., 1988. Constant rate infiltration: A versatile nonlinear model, 1. Analytic solution. Water Resour. Res., 24(1): 145–154.

Brutsaert, W., 1975. A theory for local evaporation (or heat transfer) from rough and smooth surfaces at ground level. Water Resour. Res., 11(4): 543–550.

Butters, G.L. and Jury, W.A., 1989. Field scale transportof bromide in an unsaturated soil. A. Dispersion modeling. Water Resour. Res., 25(7): 1575–1581.

Cohen, Y. and Ryan, P.A., 1989. Chemical transport in the top soil zone — The role of moisture and temperature gradients. J. Hazard. Mater., 22: 283–304.

Cohen, Y., Taghavi, H. and Ryan, P.A., 1988. Contaminant diffusion under non-isothermal conditions in nearly dry soils. J. Environ. Qual., 17(2): 198–204.

Edlefson, N.E. and Anderson, A.B.C., 1943. Thermodynamics of soil moisture. Hilgardia, 15: 31–298.

Edwards, W.M., Shipitalo, M.J., Dick, W.A. and Owens, L.B., 1992. Rainfall intensity affects transport of water and chemicals through macropores in no-till soil. Soil. Sci. Soc. Am. J., 56: 52–58.

Fletcher, C.A.J., 1991. Computational Techniques for Fluid Dynamics, 1. Springer, Berlin.

Fuller, E.N., Schettler, P.D. and Giddings, J.C., 1966. A new method for predicting binary gas-phase diffusion coefficients. Ind. Eng. Chem., 58(5): 19–27.

Gierke, J.S., Hutzler, N.J. and Crittenden, J.C., 1990. Modeling the Movement of Volatile Organic Chemicals in Columns of Unsaturated Soil. Water. Resour. Res., 26: 1529–1547.

Grifoll, J. and Cohen, Y., 1994. Chemical volatilization from the soil matrix: Transport through the air and water phases. J. Hazard. Mater., 37: 445–457.

Haan, C.T., Nofziger, D.L. and Ahmed, F.K., 1994. Characterization of chemical transport variability due to natural weather sequences. J. Environ. Qual., 23: 349–354.

Hayduk, W., Minhas, B.S. and Lan, J., 1982. Correlations for prediction of molecular diffusivities in liquids. Can. J. Chem. Eng., 60: 295–299.

Howard, P.H. (Editor), 1987. Book of Environmental Fate and Exposure for Organic Chemicals, Vol. II. Lewis, Chelsea, MI.

Howard, P.H., Boethling, R.S., Jarvis, W.F., Meylan, W.M. and Michalenko, E.M., 1991. Handbook of Environmental Degradation Rates. Lewis, Chelsea, MI.

Imhoff, P.T. and Jaffé, P.R., 1994. Effect of liquid distribution on gas–water phase mass transfer in an unsaturated sand during infiltration. J. Contam. Hydrol., 16(4): 359–380.

Jaynes, D.B., 1991. Field study of bromacil transport under continuous-flood irrigation. Soil Sci. Soc. Am. J., 66: 658–664.

Jury, W.A. and Gruber, J., 1989. A stochastic analysis of the influence of soil and climatic variability on the estimate of pesticide groundwater pollution potential. Water Resour. Res., 25(12): 2465–2474.

Jury, W.A., Spencer, W.F. and Farmer, W.J., 1983. Behavior assessment model for trace organics in soil, I. Model description. J. Environ. Qual., 12(4): 558–564.

Jury, W.A., Spencer, W.F. and Farmer, W.J., 1984a. Behavior assessment model for trace organics in soil, II. Chemical classification and parameter sensitivity. J. Environ. Qual., 13(4): 567–572.

Jury, W.A., Spencer, W.F. and Farmer, W.J., 1984b. Behavior assessment model for trace organics in soil, III. Application of screening model. J. Environ. Qual., 13(4): 573–579.

Jury, W.A., Spencer, W.F. and Farmer, W.J., 1984c. Behavior assessment model for trace organics in soil, IV. Review of experimental evidence. J. Environ. Qual., 13(4): 580–586.

Jury, W.H., Russo, D., Streile, G. and Hesam, E.A., 1990. Evaluation of volatilization by organic chemicals residing below the soil surface. Water. Resour. Res., 26: 13–20.

Karickhoff, S.W., 1981. Semi-empirical estimation of sorption of hydrophobic pollutants on natural sediments and soil. Chemosphere, 10: 833–846.

Leighton, D. and Calo, J., 1981. Distribution coefficients of chlorinated hydrocarbons in dilute air–water systems for groundwater contamination applications. J. Chem. Eng. Data, 26: 382.

Lyman, W.J., Reehl, W.F. and Rosenblatt, D.H., 1990. Handbook of Chemical Property Estimation Mehods. American Chemical Society, Washington, DC.

Mackay, D., Shiu, W.Y. and Ma, K.C., 1992. Illustrated Handbook of Physical–Chemical Properties and Environmental Fate for Organic Chemicals, Vol. I. Lewis, Chelsea, MI.

Millington, R.J., 1959. Gas diffusion in porous media. Science, 130: 100–102.

Nair, S., Longwell, D. and Seigneur, C., 1990. Simulation of chemical transport in unsaturated soil. J. Environ. Eng., 116(2): 214–235.

Nielsen, D.R., van Genuchten, M.Th. and Biggar, J.W., 1986. Water flow and solute transport processes in the unsaturated zone. Water Resour. Res., 22(9): 895–1085.

Nofziger, D.L. and Hornsby, A.G., 1986. A microcomputer-based management tool for chemical movement in soil. Appl. Agric. Res., 1: 50–56.

Olson, R.L. and Davis, A., 1990. Predicting the fate and transport of organic compounds in groundwater. hazard. Mater. Control, 3: 40–64.

Oppong, F.K. and Sagar, G.R., 1992. The activity and mobility of triasulfuron in soil as influenced by organic matter, duration, amount and frequency of rain. Weed Res., 32(3): 157–165.

Patel, K.M. and Greaves, M., 1987. Surfactant dispersion in porous media. Chem. Eng. Res. Data, 65: 12.

Piver, W.T and Lindstrom, F.T., 1991a. Mathematical models for describing transport in the unsaturated zone of soils. In: O. Hutzinger (Editor), Handbook of Environmental Chemistry, Vol. 5 — Part A. Water Pollution. Springer, Berlin, pp. 128–259.

Piver, W.T. and Lindstrom, F.T., 1991b. Numerical methods for describing chemical transport in the unsaturated zone of the subsurface. J. Contam. Hydrol., 8(3/4): 243–262.

Press, W.H., Flannery, B.P., Teukolsky, S.A. and Vetterling, W.T., 1989. Numerical Recipes. Cambridge University Press, Cambridge.

Rawls, W.J. and Brakensiek, D.L., 1985. Prediction of soil water properties for hydrologic modeling. Proc. Symp. Comm. on Watershed Management, Irrigation and Drainage, Div., Am. Soc. Civ. Eng. Convent., Denver, CO.

Richards, L.A., 1931. Capillary conduction of liquids through porous medium. Physics, 1: 318–333.

Rosenbloom, J., Mock, P., Lawson, P., Brown, J. and Turin, H.J., 1993. Application of VLEACH to vadose zone transport of VOCs at an Arizona superfund site. Groundwater Monit. Remediat., pp. 159–169.

Ross, P.J., 1990. Efficient numerical methods for infiltration using Richards' equation. Water Resour. Res., 26(2): 279–290.

Ruffner, J.A. and Bair, F.E., (Editors), 1987. The Weather Almanac. Gale Research Co., Detroit, MI.

Russo, D., Jury, W.A. and Butters, G.L., 1989a. Numerical analysis of solute transport during transient irrigation. 1. The effect of hysteresis and profile heterogeneity. Water Resour. Res., 25: 2109–2118.

Russo, D., Jury, W.A. and Butters, G.L., 1989b. Numerical analysis of solute transport during transient irrigation. 2. The effect of immobile water. Water Resour. Res., 25: 2119–2127.

Ryan, P.A. and Cohen, Y., 1990. Diffusion of sorbed solutes in gas and liquid phases of low-moisture levels. Soil. Sci. Soc. Am. J., 54: 312–346.

Sahimi, M., Heiba, A., Davis, H. and Scriven, L., 1986. Dispersion in flow through porous media, II. Two phase flow. Chem. Eng. Sci., 41: 2123.

Shoemaker, A.C., Culver, T.B., Lion, L.W. and Peterson, M.G., 1990. Analytical models of the impact of two-phase sorption on subsurface transport of volatile chemicals. Water. Resour. Res., 26: 745–758.

Sleep, B.E. and Sykes, J.F., 1989. Modeling the transport of volatile organics in variable saturated media. Water Resour. Res., 25(1): 81–92.

Thornthwaite, C.W., 1948. An approach toward a rational classification of climate. Am. Geogr. Rev., 38: 55–94.

van Genuchten, M.Th., 1980. Predicting the hydraulic conductivity of unsaturated soils. Proc. Soil Sci. Soc. Am., 44(5): 892–898.

van Genuchten, M.Th. and Wierenga, P.J., 1977. Mass transfer studies in sorbing porous media, II. Experimental evaluation with tritium (^3H_2O). Soil. Sci. Soc. Am. J., 41: 272–278.

van Genuchten, M.Th., Wierenga, P.J. and O'Connor, G.A., 1977. Mass transfer studies in sorbing porous media, III. Experimental evaluation with *2,4,5*T. Soil. Sci. Soc. Am. J., 41: 278–285.

Wierenga, P.J. and van Genuchten, M.Th., 1989. Solute transport through small and large unsaturated soil columns. Ground Water, 27(1): 35–42.